Experimental data and numerical modeling of flashing jets of pressure liquefied gases

Jean-marc Lacome, Cédric Lemofack, Didier Jamois, Julien Reveillon, Benjamin Duret, François-Xavier Demoulin

Experimental data and numerical modelling of flashing jets of pressure liquefied gases

Jean-Marc Lacome[a,1], Cedric Lemofack, Didier Jamois[a], Julien Reveillon[b], Benjamin Duret[b], Francois-Xavier Demoulin[b]

[a]Institut National de l'Environnement Industriel et des RISques (INERIS), Parc Technologique Alata BP, 2F-60550 Verneuil-en-Halatte,France [b]CORIA-UMR 6614-Normandie Universite, CNRS-Universite et INSA de Rouen, Campus Universitaire du Madrillet, 76800 Saint Etienne du Rouvray, France

---

Abstract

In industrial activities involving liquefied pressurized gases (LPG), there are several situations that can lead to hazardous flashing two-phase jets with toxic and explosive consequences. The objective of this study was to further our comprehension of such phenomena in order to develop tools that will enable operational decisions to be made within the framework of risk assessment. After a review of the literature on these phenomena, experimental and numerical models were applied to study the two-phase jet resulting from any LPG releases. It focuses especially on the cooling effect that was evidenced by large scale trial experiments on releases of butane and propane carried out during the Flashing Liquids in Industrial Environment (FLIE) project. For LPG release, experimental observations show that the minimum temperature values are far below the boiling temperature. Experimental evidence completed by a new dedicated numerical model (TEM: Thermodynamic Equilibrium Model) able to handle both boiling and vaporization phenomena gives a coherent picture of the two-phase flow behavior after the expansion zone. Experimental data analysis completed by comprehensive numerical simulations provides evidences that the system formed by air, vapor and liquid droplets tends to reach an equilibrium locally.

---

[1] Tel.: +33 (0) 344556134; fax: +33 (0) 344556200.

Email address: jean-marc.lacome@ineris.fr (Jean-Marc Lacome)

Keywords

toxic and explosive consequences, cooling effect, new numerical model

1. Introduction

In many industrial activities, there are several types of situations that can lead to hazardous flashing two-phase jets. The most frequent cases are jets emanating from pipe leakage or vessel failure. If high pressure liquefied gases are involved, the accidental release may result in a sudden and rapid hazardous toxic or flammable flashing two-phase jet. In such accidental releases [1, 2], it is demonstrated that the inherent casualties are observed over a large area. The loss of human life and extensive injuries may be the most dramatic consequences.

Given the toxic or flammable nature of the materials stored as pressure liquefied gases, it is important to predict these hazardous effects within the framework of risk assessment [3, 4]. Therefore, the development of numerical models able to simulate the two-phase flows resulting from breaches or leakages of a vessel containing liquefied gas is of great interest. A critical review [5] of source term modeling for toxic release scenarios of pressurized liquefied gases showed that there is "still a significant uncertainty in the overall modeling process". Indeed, several major stumbling blocks are observed as far as the modeling of suspension and evaporation of the aerosol is concerned. The characterization of the rain out region spreading on the floor is also a source of great numerical uncertainty. It is generally assumed that a two-phase flashing jet is divided into 3 parts (Figure 1): (1) the expansion region where the liquid evolves from a thermodynamic state defined mainly by the internal flow temperature and pressure to the external atmospheric conditions; (2) the entrainment region where the atomized liquid jet evaporates and mixes with the ambient air; (3) the rain-out region, which is a liquid-solid deposit of the falling jet. The droplets in this two-phase jet evaporate, leading to a continuous mixing between the ambient air leaking flow, which is colder than the air. Most of the time, a strong cooling effect is observed. It may have some influence on the general behavior of both free and impinging jets [1, 6].

To study such complex and coupled phenomena, experiments and modeling approaches are required. In the first part of this paper, the physical behavior of flashing jets is explored from the description based on the original experiments

performed at INERIS as part as the FLIE (Flashing Liquids in Industrial Environment) European collaborative project [7] that aimed to study hazardous flashing jet releases. The analysis focuses especially on the cooling effect that was shown by large scale trials experiments carried out on releases of butane and propane. In as second part, this paper first describes a CFD modeling study carried out by means of a usual spray model followed by a detailed description of a new vaporization model and comparisons with experimental results.

1.1. Large-scale experimental flashing jets

1.1.1. Large-scale experimental facilities

Within the framework of the FLIE project, an experimental campaign of jet release test cases was performed by INERIS [7] and VKI [8]. Nearly one hundred experiments with horizontal jet (free jets but also impinging jets by introducing obstacle at a maximum distance of 2 meters from the release point) were performed with LPG at ambient temperature with a regulated pressure ranging from the minimum saturation pressure up to $15\mathrm{bars}$ with an orifice (circular or rectangular shape) of an equivalent diameter from $10\mathrm{mm}$ to $25\mathrm{mm}$. This enabled LPG gases to be studied in their usual industrial conditions, that is ambient temperature and saturation pressure for storage use or ambient temperature and saturation pressure plus some bars due to filling operations or hydraulic pressure. During releases, several parameters were recorded:

- ambient conditions: direction and speed of the wind, temperature, humidity and atmospheric pressure,
- release tank: pressure, temperature at several heights in the tank and at the liquid/gas interface, the weight of the tank (to calculate the mass flow rate),
- release point: pressure and temperature inside the flexible pipe just before the exit to assess the friction loss,
- inside the jet: a dual phase Doppler anemometer [9] allows measured (axial and vertical velocity) speed and size of droplets at several locations in the jet; temperature thermocouples were located inside the jet,
- rain out: six bonds equipped with continuous weight measurements were used to study the phenomena of liquid pool formation,
- obstacle: six surface temperature thermocouples.

The measurements of rain out have already been investigated and published [10]. Temperatures inside the jet were measured using type K thermocouples. To mitigate the possible accumulation of ice, small thermocouples (small needle size) were used for the large-scale tests. Figure 2 presents the positions of the thermocouples that were located on three horizontal lines of measurements placed in a vertical plane passing through the jet axis: the upper thermocouple line (Th1-Th6), the central thermocouple line (Th7Th12) and the bottom thermocouple line (Th13-Th18). To figure out the respective positions of the thermocouple and the spray, a temperature field obtained by one of the numerical models described in the second part of this article was used as background picture. Table 1 lists six cases of butane free jet experiments with temperature measurements that are analyzed in the following section. Note that cases 1 and 2 were identical in order to test reproducibility.

1.1.2. Temperature analysis of flashing jets

The difficulty in interpreting measurements, as underlined by Allen et al. [11], arises from the intrusive nature of the measurement techniques. Among intrusive techniques, comparing temperatures obtained with a rack of thermocouples or with single thermocouple wires [12] of different types leads to relatively similar results. Among non-intrusive techniques, Kamoun et al. [13] have recently used the Global Rainbow Technique (GRT) to measure temperature and droplet size. Results are consistent with previous experiments carried out with this non–intrusive technique [14]. However, both intrusive and non-intrusive techniques may display some unexplained discrepancies when comparing temperature evolution measured within the jet by GRT and classical thermocouple measurements [12]. Measuring of temperature within a flashing jet remains an issue of primary importance, which is not fully resolved. However, comparisons between measured data and CFD modeling [15] enhance the understanding of the physical phenomenona that drive the temperature evolution. Table 1 presents the different parameters concerning the FLIE test cases of butane release. The mass flow rate at the orifice for each release was roughly estimated by using Bernoulli's law in order to assess the level of sub cooling of the releases. It gives:

$$G_b = C_d \frac{\pi D^2}{4} \sqrt{2\rho_{lo}(P_o - P_e)} \quad , \tag{1}$$

where G_b (kg/s) is the mass flow rate and C_d (dimensionless) is the discharge coefficient through the constriction. It is set to $C_d = 0.62$ which is a typical value

for this kind of orifice, the diameter is D (m). P_o is the pressure (Pa), measured inside the LPG flexible pipe (just before the exit), that drives the butane flow outside where the pressure, P_e (Pa) is equal to atmospheric pressure. ρ_{lo} is the liquid density (kg/m^3) within the flexible pipe. Because of friction loss between the tank storage and the orifice, the pressure P_o measured just before the exit is lower than the tank pressure P_i. In all cases, measurement shows $k(P_o - P_i)/P_i k \leq 2\%$, except for case 4 with the largest orifice diameter where $k(P_o - P_i)/P_i k \approx 30\%$.

The ratio between the experimental mass flow rate G_{exp} and the theoretical one G_b indicates a better estimation when the liquid compression rate (P_o/P_{sat}) is high. As its definition is similar to the sub-cooling rate, it will be denoted as such.

Figure 3 displays the time averaged temperature profiles along the jet corresponding to the cases in table 1. The first two reference cases (1 and 2 in table 1) have initially identical conditions. Since identical results are observed, it demonstrates the replicability of the measurements.

It can be seen that the minimum temperature values go below the boiling temperature of butane ($T_{boiling} = -0.5\ ^\circ C$ at 1atm). The same behavior is reported in a previous experiments by Allen et al. [16] and Yildiz et al. [12]. In the central jet axis, the measured temperature reaches a plateau around $-45\ ^\circ C$. This value was around $-50\ ^\circ C$ for propane test releases [17] which is consistent with the small-scale experiments carried out earlier [12, 16]. Indeed, in these previous experiments, a minimum plateau temperature was observed around $-70\ ^\circ C$ and $-55\ ^\circ C$ for propane ($T_{boiling} = -42\ ^\circ C$ at 1atm [12]) and for R134A ($T_{boiling} = -26.7\ ^\circ C$ at 1atm [16]) respectively with nozzle orifice diameters of 1 mm or 2 mm for Allen's experiments and 1 mm or 4 mm for Yildiz et al' experiments. After this plateau, the temperature increases to approach the ambient temperature T_e. This strong decrease in temperature is due to the evaporation of the droplets created by the jet fragmentation and the air engulfed into the flashing butane jet that contributes to reducing the butane partial pressure. Thus, the system formed by air, vapor and liquid droplets tends to reach equilibrium by decreasing the temperature. There is a competition between the endothermic process of droplet evaporation and warming of the whole jet by the entrained air. The spray jet cools down until liquid vaporization no longer has any influence on the flow.

Just behind the orifice, along the jet axis, the ambient air is not yet entrained in sufficient quantity to provide the energy to evaporate the droplets as air entrainment primarily occurs at the jet / air interface. Thus, its effects are more

visible in a position farther from the orifice. The distance, measured from the leaking orifice where the minimum temperature is observed, is usually named the Minimum Temperature Distance (MTD) in the literature [18]. Allen [19] assumed that this distance coincides with the limit of droplet existence. In a general review of flashing jet studies, Polanco et al. [18] mentioned that it is an important parameter defining the end of the boiling and nucleation process. Beyond this point, the temperature rises to reach the ambient temperature. Allen [19] reported that the MTD for any release ranges between $x/D = 150$ and $x/D = 170$, when expressed in a dimensionless form, but Polanco et al. [18] pointed out that it is difficult to make a conclusion about the MTD location for general cases. The dimensionless representation of all the temperature profiles measured, within butane and propane jets, during the FLIE project, provided no information about the MTD location and showed that it could not be easily predicted. It may be observed that, in the central jet axis, the MTD is higher than $1.5\mathrm{m}$.

Regarding the results in the central jet axis (Fig. 3-center plot), further comments can also be made regarding the starting point of the temperature increase. It can be clearly seen that the position where the jet temperature starts to increase after the MTD plateau goes further downstream as the mass flow rate increases, since the higher the mass flow rate, the greater the amount of entrained air required to evaporate the droplets. Simulations presented in the second part of the present paper provide evidence, in particular about the butane liquid mass fraction, that confirms this first hypothesis. The video recording of the experimental results shows that butane jets are composed of a two-phase mixture until a distance greater than the MTD is reached. However, it is impossible to distinguish water plume (condensation from wet ambient air) contributions from butane droplets.

It appears that although the total mass flow rate is about the same for several jets (cases 1, 2, 3, 4), its temperature evolution can differ according to the orifice size. The same kind of observation was described by [17] to interpret propane experimental tests performed with several orifice shapes. Slower temperature increases were also systematically observed along the center axis of propane jets, for rectangular injectors that are expected to produce more open jets than in the case of a circular orifice. Some of the measurements carried out on the upper thermocouple line (Fig. 3-top) are likely to correspond to regions that are not located within the jet. Thus, for those regions, the measured temperatures are close to the ambient temperature. For cases 4 and 5, the cooling phenomenon is pronounced. In comparison with the central thermocouple line,

the main difference is that these thermocouples are closer to the interface of the liquid jet with air. Consequently, the phenomenon of air entrainment is more pronounced and the MTD is around $1\mathrm{m}$. In the lower part of the jet (Fig. 3-bottom), when moving away from the release point, most of the measured temperatures remain below the ambient temperature, generally without any noticeable variation. Since the jet is falling, all the bottom thermocouple line is located deep within the jet where the flow is cooling down. In addition, close to the ground, exchanges between the jet and external air are probably reduced.

Due to the observed reproducibility of the measurements that indicates the same minimum temperature value for a given product, it is worth analyzing whether this temperature corresponds to an equilibrium temperature and, in this case, if there is a simple way to predict it. Previous papers [6] discussed this issue and predictions of an equilibrium temperature showed good agreement with measured cool-down temperatures. Starting from a temperature within what is commonly assumed to be the boiling point with no air entrainment, the liquid temperature decreases according to the vaporization process and the warming of the whole jet by the entrained air. When air entrainment is prevalent enough to stop the temperature falling, a quasi-steady vaporization process can be observed. For liquefied gas, the literature review shows that this value is far below the boiling temperature since the gap is about $30\ ^\circ\mathrm{C}$ as observed for propane [12, 16].

To assess this temperature gap, Fauske and Epstein [6] proposed an approach based on a quasi-steady hypothesis which assumes that the global heat transfer rate to the liquid is equal to the vaporization energy rate. This approach make it possible to assess the uniform equilibrium temperature of the jet T_{eq}. Predicted values of T_{eq} for propane, butane and ammonia were compared to the minimum temperature measured, T_{exp}, during corresponding FLIE tests. These comparisons (Table 2) show a fairly good agreement between T_{eq} and T_{exp} for butane ($-38.5\ ^\circ\mathrm{C}$ vs $-45\ ^\circ\mathrm{C}$) and ammonia ($-69.5\ ^\circ\mathrm{C}$ vs $-60\ ^\circ\mathrm{C}$) test releases. On the other hand, the case of propane shows a larger discrepancy ($-79.5\ ^\circ\mathrm{C}$ vs $-50\ ^\circ\mathrm{C}$). It should be kept in mind that the LPG used during the FLIE project was commercial LPG, thus the composition of propane may have included a volume fraction of butane up to 19%. It should be simply assumed that, because of the more rapid vaporization rate of propane, there is no time to reach equilibrium before complete evaporation of the liquid. For propane and ammonia, predicted equilibrium temperatures are below measured 'cool down' temperatures; this observation seems consistent with the physics. Indeed, the simple approach

ignores potential heat sources such as, for example, water condensation (ambient air humidity) within the jet, which reduces the cooling effect.

2. Numerical modeling

The purpose of this work is to set up a numerical model to address the simulation of a leakage from a tank of liquefied pressurized gas. As a first stage, selected approaches available in the literature are briefly reviewed and applied in a simulation of the butane experiment described above. The results highlight some issues regarding the transition between boiling and vaporization processes. From this finding, a new strategy is developed to determine heat and mass transfer. Finally, a new model is applied to simulate a butane release experiment. Results of the model are discussed and compared with experimental data in order to test the model hypothesis. Globally the general behavior of the simulated spray compares well with available experimental data.

2.1. Expansion region models

The expansion zone corresponds to the transition from internal flow up to the very near field where the liquid pressurized gas is released. Current numerical simulations do not consider all the physical aspects that can be encountered during the release of a liquefied gas. Accounting for all of them in a single model would be too complex and computationally too costly. Consequently a combination of strong simplifications based on experimental measurements is generally used and, in accordance with previous studies [20, 5, 15], the present approach to liquefied gas leakage relies on phenomenological and theoretical investigations.

To mimic the flash boiling phenomenon that occurs at the orifice exit down to the end of the expansion region, where the pressure of the flow reaches the atmospheric pressure, the flow is first considered to be homogeneous but with the possibility of liquid/gas equilibrium in accordance with thermodynamic laws. The general properties of the fluid are obtained by means of a weighting operation between the gas and the liquid. This assumption is also used within homogeneous equilibrium models, detailed later, to calculate the mass flow rate [5]. Because of the homogeneity hypothesis, gas and liquid have the same velocity and the same temperature which is determined by considering a thermodynamic equilibrium between the two phases. This description assumes that the flow reaches equilibrium quickly during the expansion phase. Once at atmospheric pressure, the flow temperature is expected to be equal to the

boiling temperature at the end of the expansion zone. Heat and mass transfer with the external environment is assumed to be negligible due to the very short time scale involved in the phase change process. The portion of air entrained into the two-phase jet near the orifice is then neglected. With this assumption models are thus mainly based on mass, momentum and energy balances [21, 22] during the jet expansion process. Within this framework there are still several choices for modeling the expansion zone, each based on a different approach to estimate the final thermodynamic and dynamic states. These approaches are now described.

The acceleration of the flow at the breach is the consequence of the sudden drop in pressure. Measurements of pressure and temperature at the release point (non-affected position just before the breach where pressure and temperature are P_0 and T_0, respectively, (Fig. 4)) are taken as starting points for the models. From this position, the flow, which is mostly liquid except for the residual gas, experiences a sudden drop in pressure down to its saturation pressure between the release point and the breach. Since this event happens suddenly, it is considered that the temperature remains constant. These conditions characterize the expansion zone initiation, i.e., any additional decrease in pressure would promote a phase change and thus flow expansion. This stage is referred to as point $()_b$ (breach) where the temperature is $T_b = T_0$, the pressure is the related saturation pressure $P_b = P_{sat}(T_b)$ and the corresponding density is noted ρ_b. Considering the measured mass flow rate and the known diameter of the orifice (breach) at the end pipe section, the velocity u_b is easily determined. The output properties of the expansion zone, denoted $()_{ex}$ have to be determined from these breach conditions. The different locations described here are shown in the sketch in figure 4. A complete CFD simulation of the expansion is beyond the scope of the present work, which focuses on the dispersed flow evolution after the expansion. Consequently, three modeling proposals, based on the literature, were considered in the present work to mimic the expansion zone evolution.

The first one is called HEM for Homogeneous Equilibrium Model. It relies on simple physical assumptions. Firstly, the velocity u_{ex} at the end of the expansion zone is assumed to remain equal to u_b assuming that phase change leads mainly to an expansion of the flow in the radial direction without accelerating the remaining liquid jet noticeably. The pressure P_{ex} has reached the atmospheric pressure P_{atm} and thus, the temperature is the corresponding liquid saturation pressure $T_{ex} = T_{eb}(P_{atm})$. The vapor mass fraction, $Y_{v,ex}$, is approximated by assuming that the energy lost by the liquid during the temperature drop $\Delta T = (T_b$

$- T_{ex}$), is entirely due to evaporation of the liquid.It leads to the simple relation $Y_{v,ex} = C_p \Delta T / L_v$.

This simple model was used in this study, where an essential parameter such as mass flow rate is known, and compared with the ATEX (ATmospheric EXpansion) models [22]. These models also calculate the final conditions $()_{ex}$ at the end of the expansion zone from the initial conditions at the breach $()_{br}$. The final conditions are composed of five unknowns: the surface area A_{ex}, the flow velocity u_{ex}, the thermodynamic state characterized by the enthalpy h_{ex}, the density ρ_{ex} and the remaining amount of liquid $Y_{l,ex}$. Along the expansion zone, a one-dimensional homogeneous flow is assumed in thermal equilibrium with zero air entrainment. Most of the equations resolved by the two ATEX models to find the unknown data are very similar. Their common basis is the expression of the conservation of mass,

$$\rho_{ex} A_{ex} u_{ex} = \rho_b A_b u_b \quad ,$$

and the energy equation

$$\rho_{ex} A_{ex} u_{ex} \left(h_{ex} + \frac{1}{2} u_{ex}^2 \right) = \rho_b A_b u_b \left(h_b + \frac{1}{2} u_b^2 \right) \quad ,$$

while the equation of state allows for the determination of the density

$$\rho_{ex} = \rho_{ex} (P_{atm}, T_{ex}, Y_{l,ex}) \quad ,$$

and the enthalpy from both the liquid and vapor state:

$$h_{ex} = Y_{l,ex} h_L (P_{atm}, T_{ex}) + (1 - Y_{l,ex}) h_V (P_{atm}, T_{ex}) \quad ,$$

where h_L and h_V are the specific liquid and vapor enthalpies, respectively. From this common basis, two ATEX sub-models can be distinguished. The first one, ATEX MME (Mass, Momentum, Energy), uses momentum conservation :

$$\rho_{ex} A_{ex} u_{ex}^2 = \rho_b A_b u_b^2 + (P_b - P_{atm}) A_b \quad ,$$

while ATEX MEE (Mass, Entropy, Energy) is based on entropy conservation :

$$s(P_{atm}, T_{ex}, Y_{l,ex}) = s(P_b, T_b) \quad .$$

2.2. Inlet condition for entrainment zone

The objective is to apply the CFD model to the large scale jet butane experiments carried at INERIS during the FLIE project. The numerical software used for this study is the package FIRE V8.41 (AVL). The reference experimental test case chosen for simulation corresponds to a butane jet with an injection

pressure of 8 bar. Input data for this test case were taken from the experiments referenced as cases 1 & 2 (the same conditions) in the first part of the present paper. In this experiment, butane is driven to the external air for experimental purposes through a flexible pipe with a breach orifice of $10\mathrm{mm}$ in diameter. Following previous numerical work [20], a Euler-Lagrange approach for this two-phase simulation was adopted. This approach requires a diluted spray, thus it is necessary to start the jet simulation from the end of the expansion region, where flash atomization has already occurred. The corresponding computational domain is shown on figure 5.

The spray simulation requires setting the droplets characteristic in terms of diameters and velocity. These two parameters are the outcome of the atomization for which no completely established model yet exists, especially for flashing jets. To obtain some information, an additional experimental campaign was performed.

Conditions at the end of the expansion region of case 2 are summarized in table 3 for the three expansion models. Applying these models to this reference test case shows the dispersion of the condition that may be estimated at the end of the expansion zone. This shows the large uncertainty that affects the inlet condition resulting from the expansion. This is clearly a limit of the present possible approaches that can only be overcome by additional investigation on the zone that covers the injector flows and the expansion zone both experimentally and numerically. These will be the main directions of further work.

For the time being, a reference case was defined and a sensitivity analysis of the main parameters was conducted to estimate which one is the most influential and whether it is possible to retrieve the global behavior of the flow as measured through the set of thermocouples. The HEM was used as reference test case to determine inlet conditions: butane quality, end of expansion region diameter, temperature and velocity. The mean droplet diameter was set to 100 μm with a spray angle of 10^o. From the previous hypotheses, the simulation concerns an atmospheric two-phase jet of butane emerging from a circular orifice that represents the end of the expansion region with a diameter of D = $63\mathrm{mm}$. The turbulence model used for this simulation is the standard k-ε model [23]. The numerical domain is presented in Figure 5. It is a 24-meter long and a 4-meter diameter cylinder. The computational domain contains about 9.10^4 mesh cells. Since the experiment was done outside, a residual wind was taken into account thanks to a co-flow of air surrounding the spray injection. The co-

flow velocity is $1\mathrm{m/s}$ with 10% of turbulence intensity, the turbulent integral length scale of which is $5\mathrm{cm}$. The external air temperature is $23^{o}\,\mathrm{C}$.

Experiments on flashing jets of liquefied gas have shown the complexity of the turbulent liquid-gas flow in strong interaction with its environment through heat and mass transfers. No simple quantitative correlation has emerged yet from experimental results to characterize the region where the cooling effect may occur. From these well-defined reference test case conditions, the next part of this study is devoted to evaluating the capacities of numerical simulation for this kind of flow with the aim of predicting temperature evolution within butane flashing jets.

The boundary conditions for case 2 are recapitulated in Table 4.

2.3. Entrainment region

2.3.1. Evaporation models

Most vaporization models in the literature are based on the Spalding analysis [24, 25] developed for a spherical droplet. Among these Spalding derived models, the one proposed by Abramzon and Sirignano [26] is a reference. It was used in this study to express the rate of vapor from a liquid droplet with a diameter a:

$$\dot{m} = \pi \rho_g D_g a Sh_c \ln(B_M + 1) \quad , \tag{2}$$

where $\rho_g D_g$ is the constant product of the carrier gas density with diffusivity while Sh_c is the convective Sherwood number. B_M is the mass transfer number :

$$B_M = \frac{Y_{v,s} - Y_{v,\infty}}{1 - Y_{v,s}} \quad , \tag{3}$$

where $Y_{v,s}$ and $Y_{v,\infty}$ are the vapor mass fraction at the droplet surface and beyond the mass transfer boundary layer, respectively. By considering the heat flux reaching the droplet surface and the energy necessary to evaporate the droplet, it is possible to express the liquid heat flux [26] :

$$Q_l = h_c \pi a^2 (T_\infty - T_s) - L_v \pi \rho_g D_g a Sh_c \ln(B_M + 1) \tag{4}$$

However thermodynamic conditions at the end of the expansion region are very particular in the case of flashing jets. The thermodynamic equilibrium assumption means that the liquid and gas temperatures are both equal to the boiling temperature. Consequently, at the surface there is only vapor $(Y_{v,s} \approx 1)$. Additionally, the gases surrounding the droplet are composed of pure vapor only $(Y_{v,\infty} \approx 1)$. This is a limit case between boiling and vaporization since any increase in temperature would promote mass transfer by boiling, while any change of gas

composition by external air dilution would promote vaporization. In this configuration, the definition of B_M given by equation 3 leads to an indeterminate formulation, thus this modeling approach is not able to determine which process has to be considered depending on the flow conditions. Since, far away from the expansion region, dilution by the air environment is expected, it is appealing to keep a standard vaporization modeling and to assume that the gases surrounding the liquid surface always contain a residual proportion of gas that is not vapor. This is achieved by considering a non-unitary maximum value for both vapor mass fractions: $(Y_{v,s} = 1 - \varepsilon_Y)$ and $(Y_{v,\infty} = 1 - \varepsilon_Y)$, with ε a small value for instance $\varepsilon_Y = 1e{-}2$. It can also be assumed that simulation starts when some air has already penetrated the jet after the expansion to justify this modification. Then, by adopting this strategy, the entrainment region can be simulated [20]. In accordance with this assumption, we initially used a similar approach in the context of the previously described butane experiments.

The results obtained using this approach were very unstable. With present conditions, it appears that the limit values of the vapor mass fraction, used to prevent an indeterminate Spalding number, becomes a key parameter. This underlines the need to modify the vaporization model to prevent any indetermination and to build a model that can handle both vaporization and boiling processes.

2.4. Thermodynamic Equilibrium Model (TEM)

The objective is to build a robust vaporization-boiling model able to self-determine the evolution of the multiphase flow starting from the end of the expansion zone. This model is then tested against previously described experimental data.

2.4.1. Principle of the TEM model

A robust mass transfer model should handle both vaporization and boiling processes. The mathematical difficulties encountered in the determination of the Spalding mass number are due to the particular inlet condition that belongs in fact to the end of a "boiling" zone. From the end of the expansion zone, liquid and gas regions are both at saturation and at boiling conditions. Considering boiling phenomena, any heat flux coming from outside should promote a phase change proportional to the heat flux divided by the latent heat of vaporization. Accordingly, the liquid heat flux $Q_l = 0$ and from equation (4), the mass transfer rate reads:

$$\dot{m} = h_c \pi a^2 (T_\infty - T_s)/L_v \quad (5)$$

This equation can determine rate transfers only in the boiling condition since no effect of the vapor concentration in the gas taken into account. The advantage of this formulation is that it does not require the determination of the Spalding number (3) which is indeterminate in this case. However, any dry air coming from outside toward the liquid surface requires a change in the model representation from boiling phenomena to vaporization phenomena in order to use equations (2-4). It requires the determination of the mass Spalding number B_M. This change of physical process expresses the competition between heat transfer and air mass transfer at the droplet surface. We tested the possibility of combining these two models but the criterion to change from boiling to vaporization representation depends on the minimum value of the air mass fraction at the surface used to switch from one model to the other. This dependency led to unstable results. Thus, to build a more robust approach, we should rely on the thermodynamic equilibrium that can be determined from any initial state characterized by a given amount of energy, liquid mass, vapor mass and air mass. The thermodynamic system at its initial state is defined by liquid mass fraction and vapor mass fraction in the presence of another gas such as air. The initial liquid temperature may differ from the vapor temperature. As in HEM model, we consider the thermodynamic equilibrium model in the final state. Equilibrium is determined assuming an ideal gas law, total mass conservation, liquid + vapor mass conservation and enthalpy conservation. For a two-phase flow (composed of liquid and gas), the determination of the equilibrium state leads to two possible scenarios: on the one hand, there remains liquid and the equilibrium is characterized by a vapor pressure equal to the saturation vapor pressure; on the other hand, only gas remains, and the quantity of vapor corresponds directly to the sum of the quantities of vapor and initial liquid. The choice of the final scenario depends on the amount of energy initially available. If it is large enough it will allow the total vaporization of the liquid.

To test the equilibrium model with the butane properties in conditions close to those of INERIS experiment an initial mixture composed of liquid butane and air was studied. The initial temperature for both liquid butane and dry air was set to 293.15 K. The equilibrium state was then studied as a function of the initial mass fraction of liquid. The pressure remains constant at $0.1\mathrm{MPa}$.

Figure 6-(a) shows the equilibrium vapor and liquid mass fraction of butane obtained at final equilibrium state (Y^*).

Even with an initial mixture full of 100% liquid butane ($Y_l^0 = 1$), there is at the equilibrium state a certain amount of vapor. This is due to the initial temperature that is above the boiling temperature ($T_b = 272.6\mathrm{K}$) at this pressure. As the initial amount of butane decreases, there is a decrease in the amount of the liquid butane at equilibrium. Eventually for $Y_l^0 = 0.2$ all the liquid butane can be vaporized. The amount of butane vapor increases first as the initial amount of butane increases but at a high amount of liquid butane it then decreases due to the thermal effect.

In figure 6-(b), the equilibrium final temperature is plotted as a function of the initial liquid butane mass fraction. For the highest concentration of liquid butane, initial value $Y_l^0 = 1$, there is no air. Since the initial temperature is set above the boiling temperature, the final mixture at equilibrium can only be composed of vapor and liquid butane. Accordingly, saturation is achieved at boiling temperature. The percentage of vapor depends on the amount of superheat and thus on the initial temperature. Note that for a sufficiently high initial temperature all the liquid should have been vaporized. For less liquid butane in the initial mixture ($Y_l^0 < 1$) a certain amount of air is present. Thus, it is the partial pressure of butane vapor that should be adapted to obtain saturation at equilibrium. From this initial condition the equilibrium temperature is necessarily less than the boiling temperature, since at equilibrium, the boiling temperature would imply partial pressure of vapor equal to the total pressure with no air in the gas phase. Indeed, the final equilibrium temperature can decrease significantly below the boiling temperature with a minimum temperature ($T^* = 228K$) obtained for $Y_l^0 = 0.2$ where there is enough initial dry air to promote complete vaporization of the liquid butane. For less initial liquid butane ($Y_l^0 < 0.2$) the butane is always completely vaporized, but since there is also less energy consumed by the vaporization of the reduced amount of liquid butane the equilibrium temperature is finally higher. This simple example shows the quite complex nature of the vaporization problem that has to be solved to deal with heat and mass transfer during the dispersion of a leakage of liquid pressurized gas. It would be interesting to consider also the presence of water vapor in the mixture that is initially present in the air. In principle, a model based on vaporization rate or boiling rate as discussed above can be applied to compute the final equilibrium state. The problem is to set up a model that covers the whole range of application namely boiling and vaporization phenomena. Up to now based on the equilibrium model only the final equilibrium state is considered. Thus, to retrieve a rate of vaporization, it has been proposed to consider that only part of the mixture achieves the equilibrium state. It is

assumed that on both sides of the liquid-gas interface a mixing layer grows and that the equilibrium state is achieved within the mixing layer. The ratio of volume cover per this mixing layer with respect to the total volume is called β, this is the equilibrium mixing volume ratio. It is possible to define and compute the evolution of this ratio to address simple cases such as evolution of the D-square law or to find results compatible with the previously referenced Abramzon and Sirignano model [26].

Determining the volume that is actually at equilibrium consists in multiplying the surface of the liquid by a certain thickness which corresponds to a boundary layer of fluid at the state of equilibrium and which develops starting from the surface according to the conditions of flow. The amount of local interface in the flow can be determined from the equations developed in the context of atomization for interfacial area density [27, 28, 29, 30]. The actual derivation of such an equation is still an active topic of research. For the present work a constant value of β was used. The principle of this approach is to base the rate of heat and mass transfer on the current state of the mixture but also on the final equilibrium state. This is unusual when compared to the standard vaporization model, such as the aforementioned ones, where only the current state is considered to provide the rate of heat and mass transfer. The advantage of considering in addition the final equilibrium state is to ensure realizability of the result even for infinite or undefined heat and mass transfer rates.

2.4.2. Application of the TEM model to INERIS experiments

The TEM approach was applied to the reference test cases (case 1&2, see Table 1) where the previously discussed vaporization models were replaced by the TEM approaches. As a first attempt, the equilibrium volume ratio for every mesh was set to $\beta = 1$. This means that the flow is assumed to be everywhere at thermodynamic equilibrium locally.

Figure 7 represents the gas temperature after the stationary state has been reached.

Computation starts after the expansion region, where the jet - composed of liquid butane droplets and pure vapor - is injected at boiling temperature. As in the experimental results, the temperature along the jet axis falls to below the boiling temperature of butane. This cooling is due to a high evaporation rate that is stimulated by the diffusion of air close to the liquid surface of the butane droplets. At the same time, a heat flux takes place from the surrounding external air to the liquid spray but it is not sufficient initially to compensate for the latent heat of vaporization consumed by the vaporization process. Close to the

injection, along the center the temperature remains at its boiling value since the air flow takes some time to reach the jet center.

Figure 8 presents a quantitative comparison between the gas temperatures given by the computational model and the temperature measured by the thermocouples. Cases 1 and 2 correspond to similar experimental conditions but for two different experimental trials to show the repeatability of the experiments. Despite the complexity of the flow and the strong hypothesis used to describe the expansion region and to build the TEM model, the quantitative comparisons are quite satisfactory. The temperature in the simulation corresponds well to the experimental gas temperature. Moreover, despite the possibility that the thermocouples close to the injector may sometimes capture liquid droplets, the measured temperature seems to remain realistic without obvious artifacts. The main cooling process is very well reproduced by experiment and simulation both in terms of magnitude and in terms of localization. This comparison shows the complementary role of simulation and experiment in such a complex situation. Taken separately they include many uncertainties about the physical phenomena that take place in the expansion zone, but together they describe the behavior of the release of pressurized liquefied gas including complex heat and mass transfer effect realistically. Experimental data provide some insight into the real flow at the measurement location, while numerical simulation provides a more complete description in regions where no measurement is available.

Figure 9 shows a comparison between computational results and thermocouple measurements for another set of conditions, case 6 (see Table 1). With respect to the reference case, this configuration corresponds to a smaller injection diameter and to a reduced inlet pressure. Despite these important changes the numerical model is still able to reproduce the main features of the flow as they are reported from experimental measurement. In the first area, *i.e.* less than 1 meter from the injection, the temperature comparison is very satisfactory. At further distances downstream the vertical bending of the jet due to gravity is more pronounced in the numerical simulation than in the experiment. Several reasons may cause this discrepancy corresponding to the simplification used to build this model. The expansion model may underpredict the velocity corresponding to the inlet condition for the dispersion zone. Another phenomenon that has been neglected is the crystallization of the water vapor in solid particles of ice within the low temperature zone. The presence of such ice particles has been proved when studying the rain out experimentally [10]. Indeed, a deposit composed of a mixture of liquid and solid water crystals was

found on the ground during the experiment. This phenomenon is not yet taken into account in our model and could have an influence on the temperature spatial distribution. Other uncertainties exist on the spray characteristics such as the mean diameter of the droplets exiting from the expansion zone.

3. Conclusion

The present work aimed to provide new insight into the physics occurring during the release of liquefied pressurized gas. After a review of the literature on the phenomena occurring during this release, new data are reported on the measurement of temperature in the flashing jet of butane performed at INERIS. Large-scale experiments were carried out during the FLIE project which was designed to study LPG release with storage conditions representative of industrial applications. A set of thermocouples gave a repeatable and comprehensive representation of the spatial temperature distribution despite the possible perturbation of measurement due to the two-phase flow nature of the jet. The data were obtained for different injector diameters, mass flow rates and injection pressures. This database made it possible to investigate LPG release and to test specific models dedicated to flashing jets.

It appears that the sudden cooldown at the exit of the injector is the reason for the persistence of the liquid phase that has a strong influence on the dynamic of the two-phase jet. Moreover, the literature review showed how difficult it is to manage and interpret temperature measurements within flashing jets. However, similar strong cooling effects were observed between several lab scale experiments but also with large-scale experiments.

The numerical study focused on the simulation of the two-phase jet starting after the expansion zone. Accordingly, the primary atomization phenomena are not simulated directly and the model that provides the inlet boundary conditions relies on approximations of the expansion zone. Nevertheless, to test the influence of those approximations, three different approaches were used to represent the expansion zone. All of them assumed the two-phase flow to be at thermodynamic equilibrium at the end of the expansion zone. Well-established CFD vaporization models were tested but the equilibrium condition leads to a non-defined parameter such as the Spalding number. Therefore, a new formulation, based on the thermodynamic equilibrium (TEM) state, has been proposed. A method to account for the departure from equilibrium has been also considered to match standard vaporization models and to account for a finite rate of heat and mass transfer locally.

The CFD modeling results obtained with the TEM model were compared to the two-phase jet experiment in terms of temperature profiles along the vertical direction. Despite an expected two-phase flow bias on the thermocouple measurement, good agreement was found between simulated and experimental temperature. The minimum temperature within the jet, which is below boiling temperature, and the minimum temperature distance are well reproduced by numerical simulation. For these very complex flows the combination of measurement and numerical simulation gives a better understanding of the flow behavior. In particular temperatures lower than the boiling temperature were measured away from the jet center but close to the injection point. Simulations showed that this is due to the competition between heat transfer coming from the external air, which tends to heat up the jet, and the dilution of the vapor by the external dry air, which promotes liquid to vapor mass transfer and thus cools the jet down even more through the latent heat of vaporization. Thus, the more ambient air is entrained within the jet, the more evaporation occurs. As the entrained air takes some time to penetrate the jet core, the center temperature remains unchanged for a while at boiling conditions emanating from the expansion zone. On the external edge, on the contrary the dry air promotes vaporization leading to a lower temperature. Globally, near the injection orifice, the vertical temperature profile has an inverse "M" shape characteristic of such phenomena. Farther downstream, there is less and less liquid to be vaporized and the heat flux coming from the external air becomes able to heat up the jet, overcoming the cooling due to vaporization.

4. Acknowledgement

The experimental projects were mainly funded by the French Ministry of the Environment and the European project FLIE. They are sincerely acknowledged.

5. References

[1] H. Lonsdale, Ammonia tank failure–South Africa, Ammonia plant safety 17 (1975) 126–131.

[2] J. Hajj, F. R.T., Failure of Tank Car TEAX 3417 and subsequent release of liquefied petroleum gas, Technical Report, National transportation safety board, 1998.

[3]]N. Nabhani, H. Mahmoodi, et A. Akbarifar, « Consequence modeling of major accidents of a real butane storage tank », Process Safety Progress, sept. 2019.

[4] X. Hu et al., « Land-use planning risk estimates for a chemical industrial park in China - A longitudinal study », Process Safety Progress, vol. 37, n° 2, p. 124-133, juin 2018.

[5] R. Britter, J. Weil, J. Leung, S. Hanna, Toxic industrial chemical (TIC) source emissions modeling for pressurized liquefied gases, Atmospheric Environment 45 (2011) 1–25.

[6] H. K. Fauske, M. Epstein, Source term considerations in connection with chemical accidents and vapour cloud modelling, Journal of loss prevention in the process industries 1 (1988) 75–83.

[7] P. Bonnet, P. Bricout, S. Duplantier, D. Jamois, J.-M. Lacome, Flashing Liquids in Industrial Environment (Flie Project) - Description of experimental large-scale phase release jets two-phase release jets, Ineris-Dra 41508, 2005.

[8] D. Yildiz, P. Rambaud, J. van Beeck, Break-up, droplet size and velocity characterizations of a two-phase flashing R134a jet, in: 5th International Conference on Multiphase Flow, Yokohama, Japan, volume 30.

[9] H.-E. Albrecht, N. Damaschke, M. Borys, C. Tropea, Laser Doppler and phase Doppler measurement techniques, Springer Science & Business Media, 2013.

[10] P. Bonnet, J.-M. Lacome, I. et des Risques, Experimental Study of Accidental Industrial LPG Releases: Rain out investigation, in: AICHE Spring National Meeting, Orlando, FL, 40th Loss Prevention Symposium, Citeseer, 2006.

[11] J. T. Allen, Characteristics of impinging flashing jets, Technical Report HSL Report No. FS/00/02, 2000.

[12] D. Yildiz, R. Theunissen, J. Van Beeck, M. L. Riethmuller, Understanding of dynamics of a two-phase flashing jet using multi-intensity-layer PIV and PDA, in: 11th International Symposium on Application of Laser Techniques to Fluid Mechanics, Lisbon, Portugal, July, pp. 8–11.

[13] H. Kamoun, G. Lamanna, B. Weigand, S. Saengkaew, G. Gréhan, J. Steelant, Temperature and droplet size measurements in a flashing ethanol jet using the global rainbow thermometry, in: ILASS Europe, pp. 1–4.

[14] J. Van Beeck, D. Giannoulis, L. Zimmer, M. L. Riethmuller, Global rainbow thermometry for droplet-temperature measurement, Optics letters 24 (1999) 1696–1698.

[15] A. Kelsey, CFD modelling of two phase flashing jets: Simulation of flashing Propane jets, Health & Safety Laboratory Report 61 (2001).

[16] J. T. Allen, Laser-based Droplet Size Measurements in Two-phase, Flashing Propane Jets, Health and Safety Laboratory (1996).

[17] P. Bonnet, P. Bricout, S. Duplantier, D. Jamois, J.-M. Lacome, Essais de rejets Diphasiques à grande échelle, Ineris-Dra 41508, 2005.

[18] G. Polanco, A. E. Holdø, G. Munday, General review of flashing jet studies, Journal of Hazardous Materials 173 (2010) 2–18.

[19] J. T. Allen, Laser-based measurements in two-phase flashing propane jets. Part one: velocity profiles, Journal of Loss Prevention in the Process Industries 11 (1998) 291–297.

[20] R. Calay, A. Holdo, Modelling the dispersion of flashing jets using CFD, Journal of Hazardous Materials 154 (2008) 1198–1209.

[21] R. Britter, Dispersion of two-phase flashing releases, Technical Report Report FM89/3, CERC Ltd, 1995.

[22] ATEX Theory Document, Technical Report, DNV Software, 2005.

[23] B. E. Launder, D. B. Spalding, Numerical simulation of turbulent flows, Computer Methods in Applied Mechanics and Engineering 3 (1974) 269–289.

[24] D. Spalding, Convective mass transfer, an introduction, Arnold, London, 1963.

[25] D. Spalding, Combustion and mass transfer: a textbook with multiple choice exercises for engineering students, Pergamon Press, 1979.

[26] B. Abramzon, W. A. Sirignano, Droplet vaporization model for spray combustion calculations, International journal of heat and mass transfer 32 (1989) 1605–1618.

[27] A. Vallet, R. Borghi, Modélisation eulerienne de l'atomisation d'un jet liquide, Comptes Rendus de l'Académie des Sciences-Series IIB. Mechanics-Physics-Astronomy 327 (1999) 1015–1020.

[28] A. Burluka, R. Borghi, et al., Development of a eulerian model for the "atomization" of a liquid jet, Atomization and sprays 11 (2001).

[29] G. Blokkeel, B. Barbeau, R. Borghi, A 3D Eulerian model to improve the primary breakup of atomizing jet, Technical Report, SAE Technical Paper, 2003.

[30] R. Lebas, T. Menard, P.-A. Beau, A. Berlemont, F.-X. Demoulin, Numerical simulation of primary break-up and atomization: Dns and modelling study, International Journal of Multiphase Flow 35 (2009) 247– 260.

case	D	T_o	P_o	$P_o/P_{sat}(T_o)$	T_e	HR	G_{exp}	G_{exp}/G_b
	mm	$^\circ C$	bar	-	$C\,\%$	%	kg/s	–
1	10	19.3	7.6	3.74	23	68	1.33	0.99
2	10	19.3	7.6	3.74	23	68	1.33	0.99
3	10	20.7	4.94	2.32	25	68	1.01	0.97
4	25	9.5	2.47	1.69	23	45.7	1.19	0.3
5	10	18.9	3.45	1.72	23	45.7	0.69	0.84
6	5	19.5	3.42	1.74	23	45.7	0.13	0.66

Table 1: FLIE test cases of butane release, D : orifice diameter, T_o : injection liquid temperature, P_o : pressure before the orifice, Psat(T_o) : saturation pressure at T_o, T_e : ambient temperature, Gexp : experimental mass flow rate, G_b : calculated mass flow rate.

Fluid	Teb($^\circ C$)	Teq($^\circ C$)	Texp($^\circ C$)
butane	- 0.5	- 38.5	≈ -45
propane	- 42.04	- 71.5	≈ -50
ammonia	- 33.43	- 69.5	≈ -60.1

Table 2: comparison between boiling temperatures at 1 atm, Teb($^\circ C$), predicted equilibrium temperatures, Teq($^\circ C$), and minimum measured temperatures (INERIS experimental trials), Texp($^\circ C$), within the jet

Analytical model	Temp. K	Pres. kPa	Vel. m/s	Mass flow rate kg/s	Vap. mass fraction	Diam. mm
Breach	292.5	203	29.6	1.33	0.04	10
HEM	272.6	101	29.6	1.33	0.16	63
ATEX-MME	272.6	101	35.6	1.33	0.16	57
ATEX-MEE	272.6	101	81.3	1.33	0.15	37

Table 3: Comparison of inlet conditions for butane jet for case 2

Variable	Inlet
Injection Diameter (mm)	63
Velocity (m/s)	29.5
Flow temperature (C)	-0.5
Ext. air temperature (C)	23
Mass flow rate (kg/s)	1.33
Vapor mass fraction (-)	0.17
Droplet D_{10} (μm)	100
Turbulent intensity (%)	10
Turb. length scale (m)	0.005
Spray angle (deg)	10

Table 4: Boundary conditions for the jet and the simulation domain

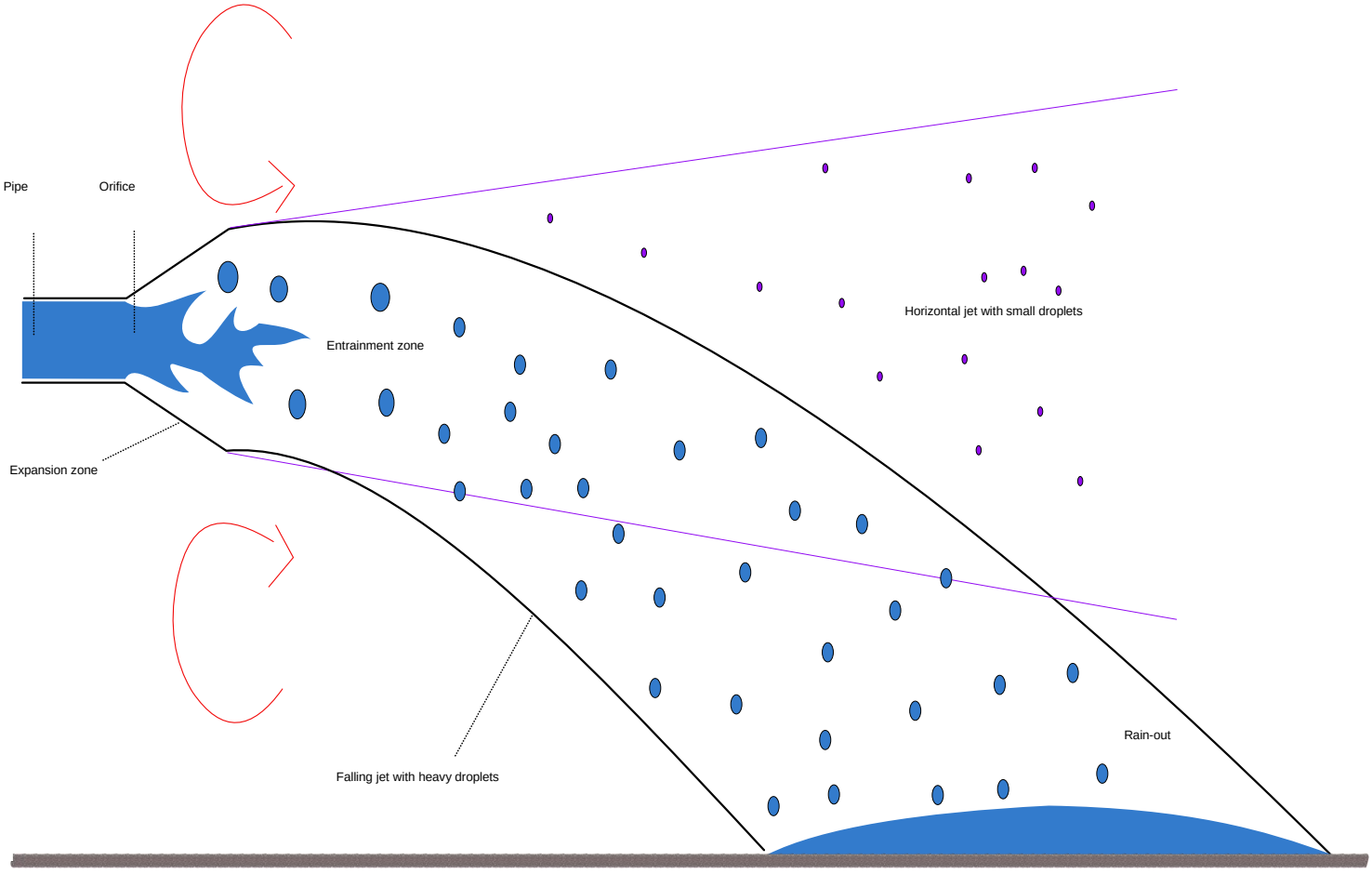

Figure 1: Schematic representation of flashing jet regions

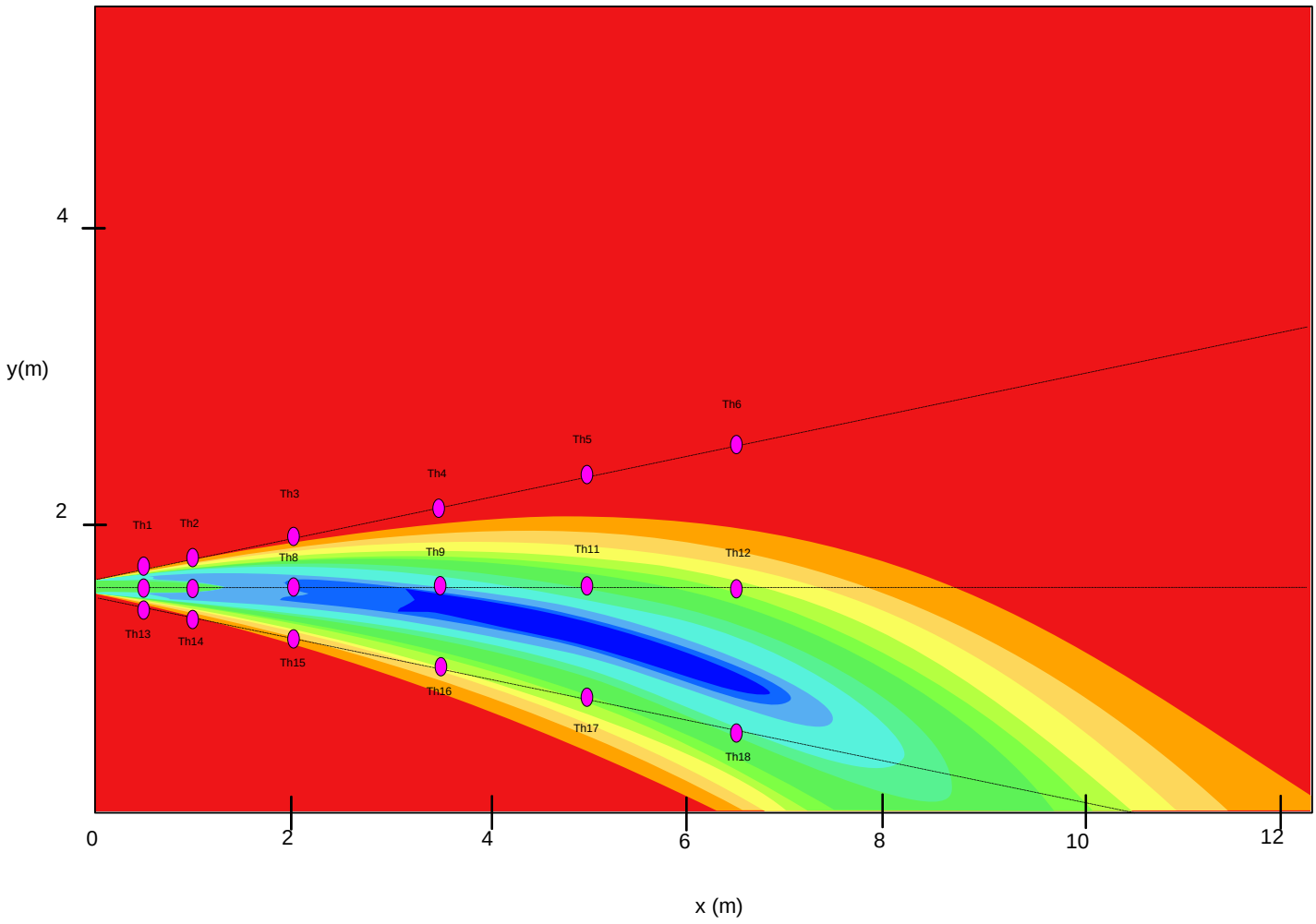

Figure 2: Vertical planar cut of the gas temperature field with thermocouple position in INERIS experiment.

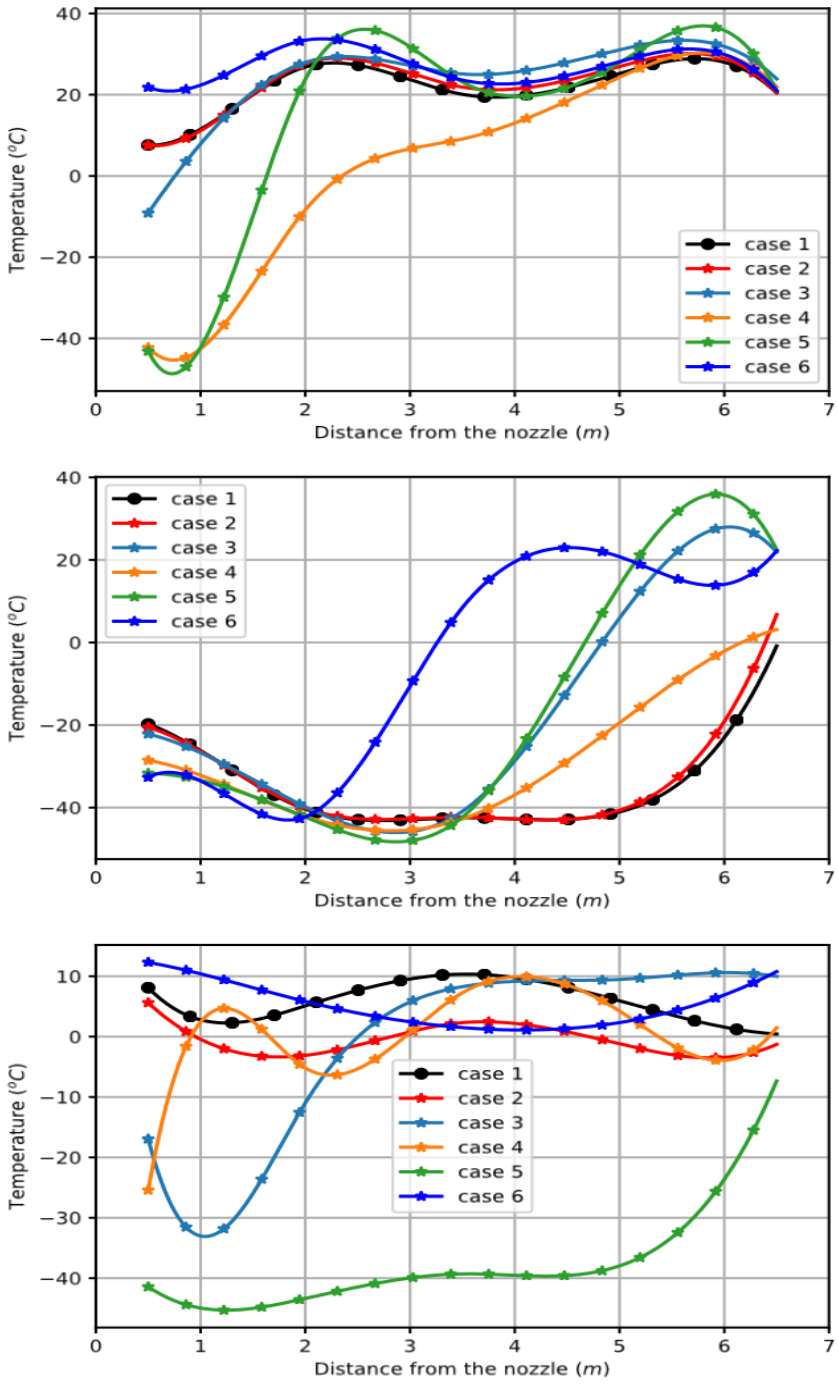

Figure 3: Temperature profiles along jet axis for six experimental releases of butanes. From top to bottom: upper thermocouple line, central thermocouple line and bottom thermocouple line.

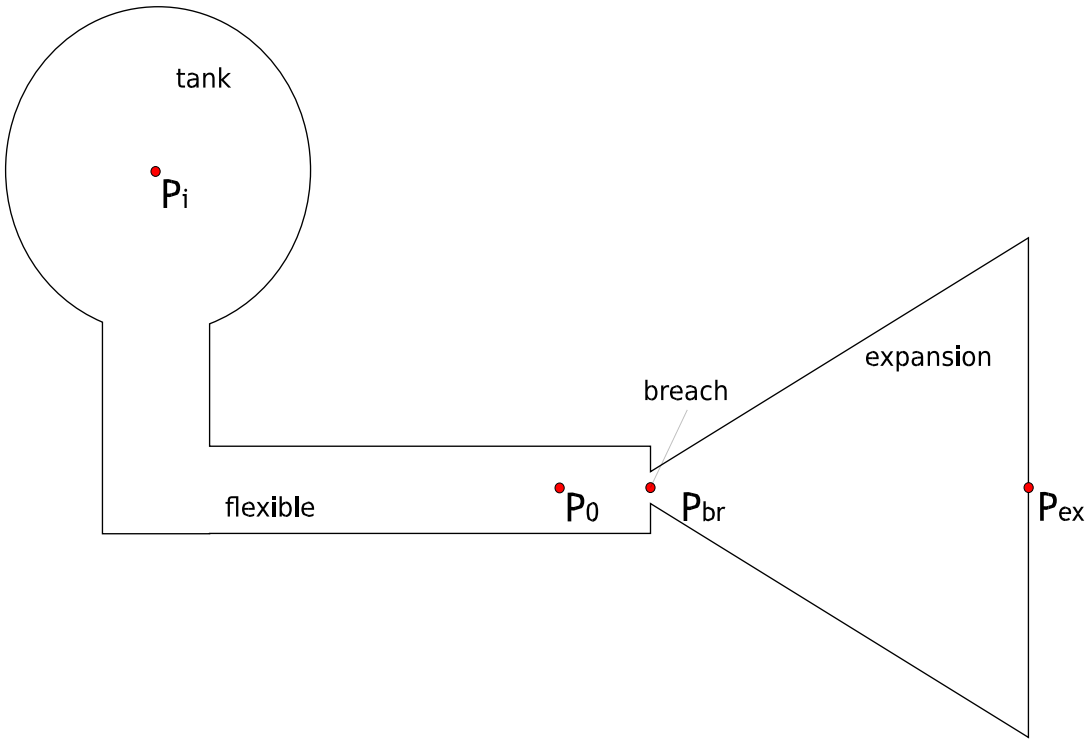

Figure 4: Schematic representation of flashing jet regions

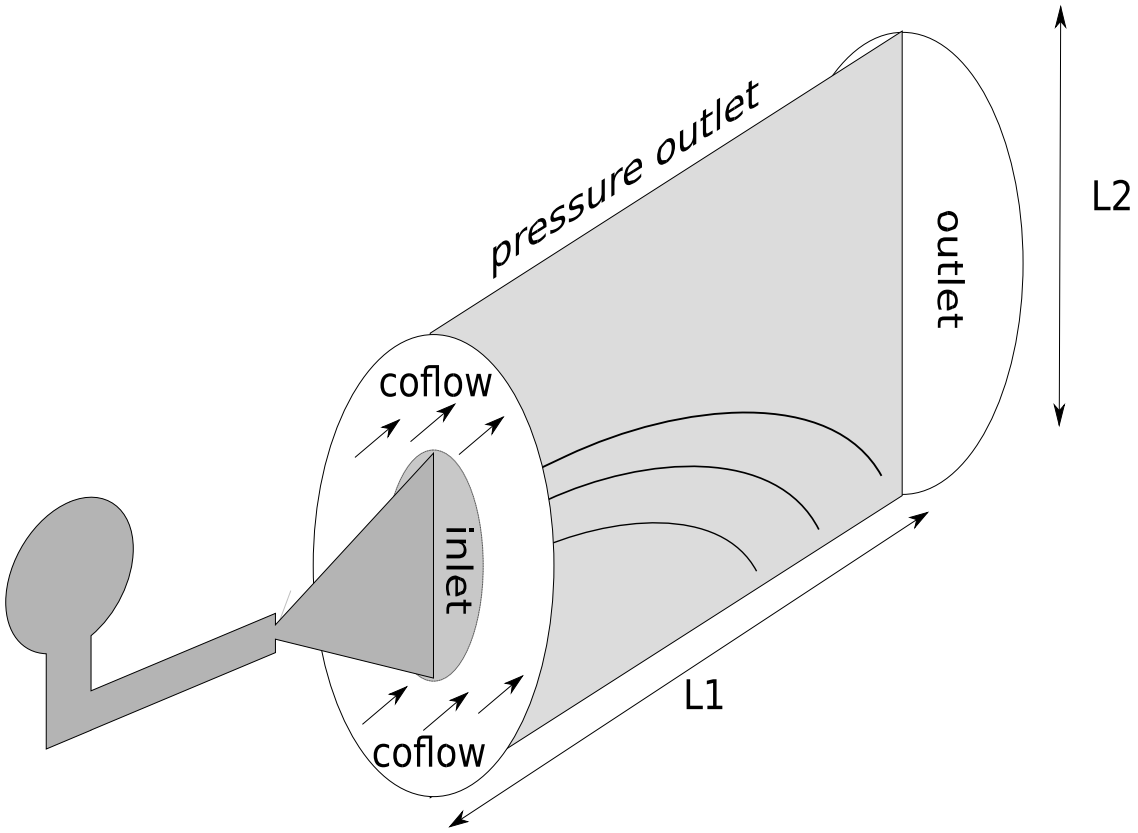

Figure 5: Computational Domain

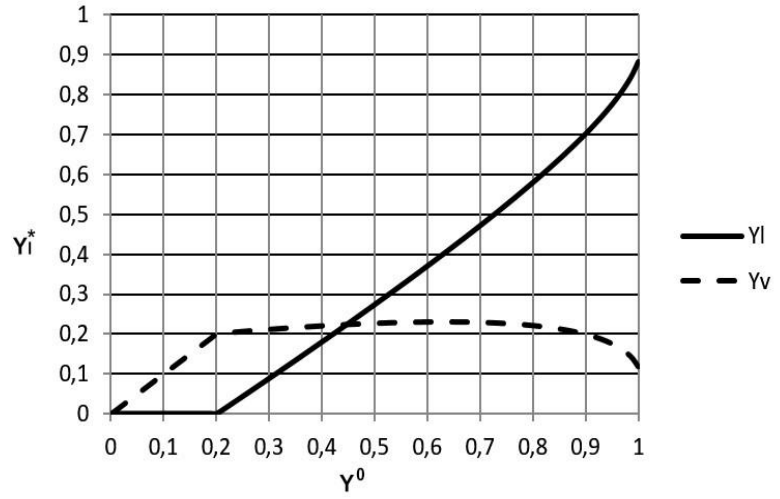

(a) - Liquid and vapour butane mass fractions at equilibrium

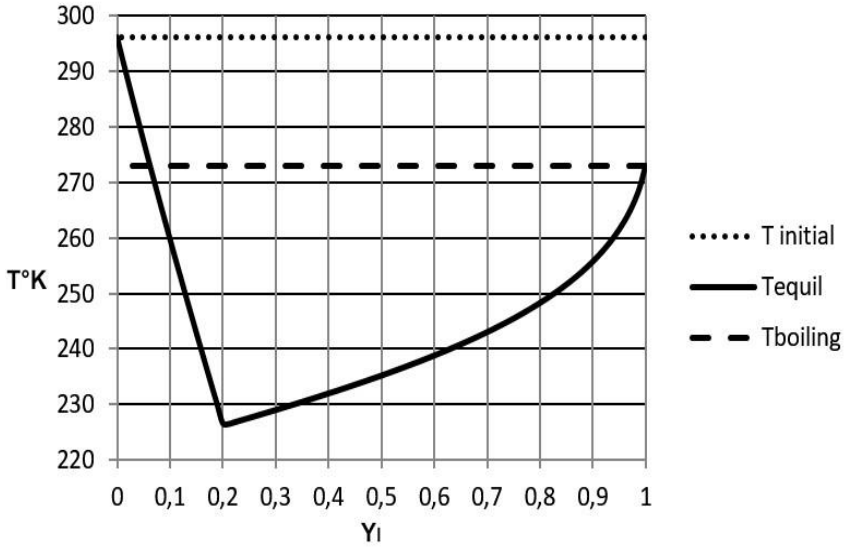

(b) - Final temperature at equilibrium

Figure 6: Final state at equilibrium for vapour and liquid mass fractions (a) and temperature (b) versus the initial liquid mass fraction of butane.

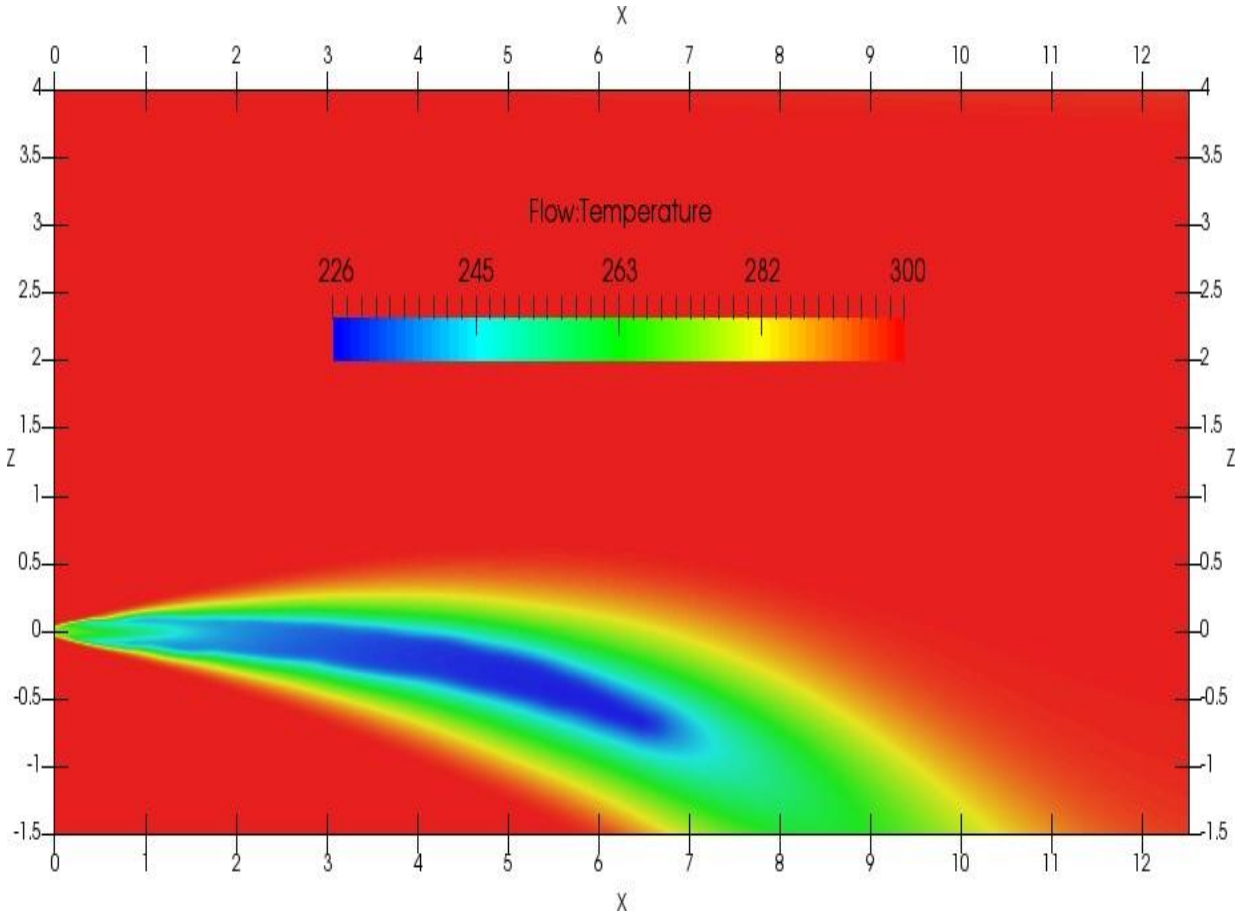

Figure 7: Temperature fields, case 2

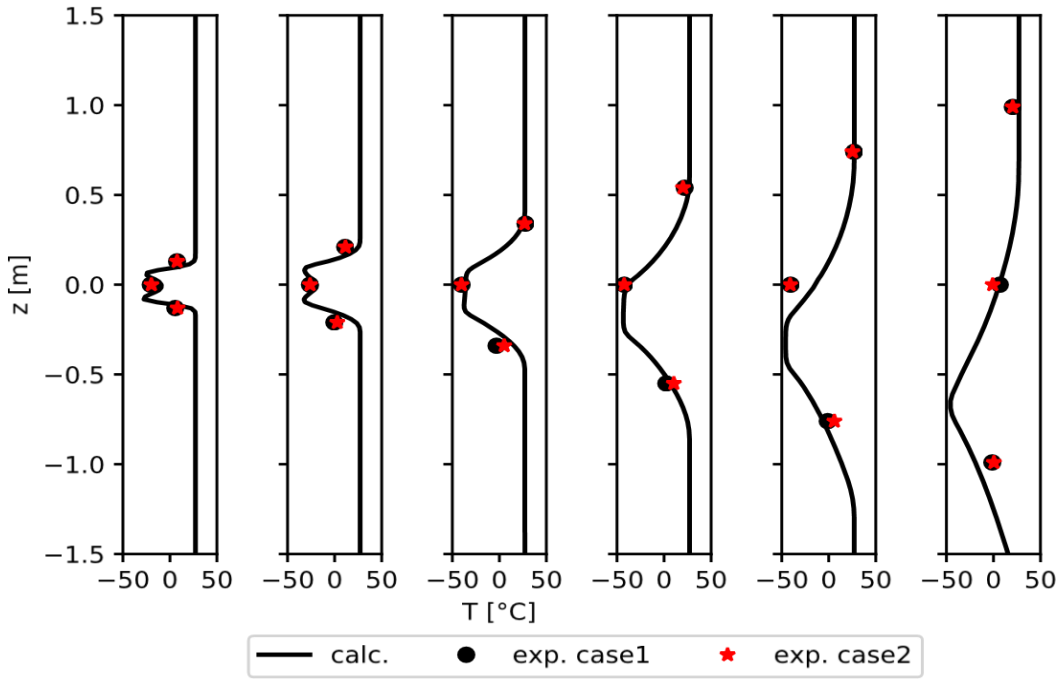

Figure 8: Comparison of several vertical profiles of temperature obtained by INERIS experiment (exp.) and the TEM numerical model (calc.) for case 1 & case 2. The axial position of the profiles from left to right are: 0.5m; 1m; 2m; 3.5m; 5m; and 6.5m.

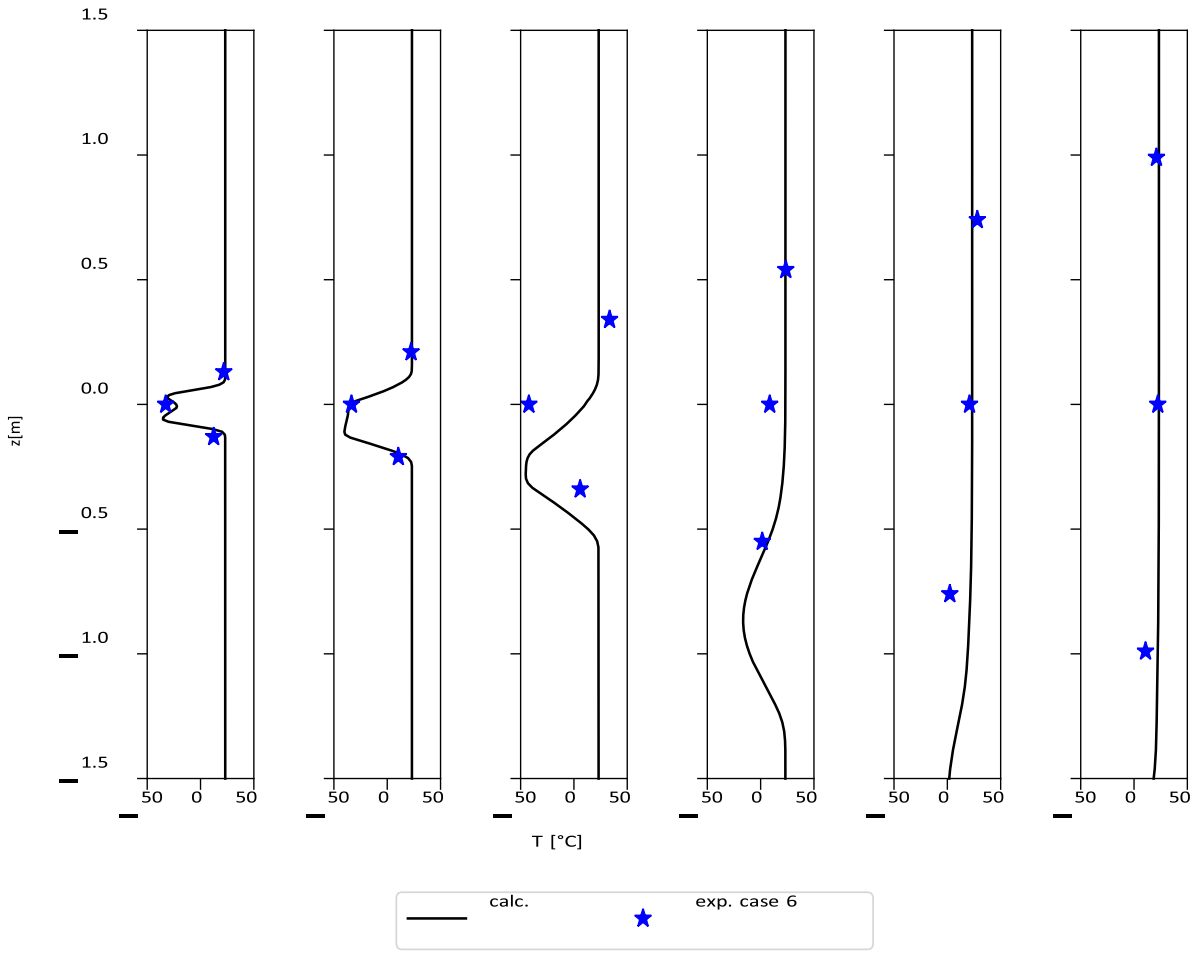

Figure 9: Comparison of several vertical profiles of temperature obtained by INERIS experiment (exp.) and the TEM numerical model (calc.) for case 6. The axial position of the profiles from left to right are: 0.5m; 1m; 2m; 3.5m; 5m; and 6.5m.